Electrical Power and Energy Systems 118 (2020) 105723

Contents lists available at ScienceDirect

Electrical Power and Energy Systems

journal homepage: www.elsevier.com/locate/ijepes

Co-optimization generation and transmission planning for maximizing large-scale solar PV integration

Mohana Alanazi[a,*], Mohsen Mahoor[b], Amin Khodaei[b]

[a] Department of Electrical Engineering, Aljouf University, Sakaka, Aljouf 72388, Saudi Arabia
[b] Department of Electrical and Computer Engineering, University of Denver, Denver, CO 80210, USA

ARTICLE INFO

Keywords:
Solar generation
Solar energy curtailment
Large-scale solar PV
Benders decomposition

ABSTRACT

The shift from conventional generation to renewable energy resources in an effort to reduce emissions has led to a rapid proliferation of renewable resources especially solar photovoltaic (PV) in power systems. More and more large-scale solar PV farms are expected to be integrated in the existing grids in the foreseeable future in compliance with the energy sector renewable portfolio standards (RPS) in different states and countries. The integration of large-scale solar PV into power systems, however, will necessitate a system upgrade by adding new dispatchable units and transmission lines. In this paper, a co-optimization generation and transmission planning model is proposed to maximize large-scale solar PV hosting capacity. The solution of this model further determines the optimal solar PV size and location, along with potential required PV energy curtailment. Numerical simulations study the proposed co-optimization planning problem with and without considering the solar PV integration and exhibit the effectiveness of the proposed model.

1. Introduction

Solar photovoltaic (PV) is considered the fastest growing renewable energy resource in the United States, with unprecedented growth at both residential and utility levels in recent years. The increasing deployment of solar PV technology is spurred by many factors such as environmental concerns stemming from global warming, falling cost of PV panels, governmental incentives, and the advances in power electronics for streamlined integration. As shown in Fig. 1, 30% of the newly added generation capacity in the U.S. in the first three quarters of 2018 came from solar with a total of 6.5 GW, 51% of it being utility-scale PV. The cumulative installed solar PV in the U.S. is currently at 60 GW and this number is expected to double over the next four years. By 2023, over 14 GW of solar PV capacity is expected to be installed annually [1]. Such large-scale solar PV integration poses multiple challenges to system control and operation due to the specific characteristics of the solar generation, including variability and uncertainty. Solar PV is considered an intermittent resource due to its output variations. Its generation is also uncertain as there is a lack of ability to perfectly predict the variations [2,3].

The integration of large-scale solar PV to the grid mandates an optimal expansion planning so the grid can sustain the maximal amount of solar PV without violating system constraints. An extensive review is conducted in the literature on the generation expansion planning (GEP) and transmission expansion planning (TEP). In GEP, the existing system is expanded to meet the future demand growth by satisfying the system reliability criteria while considering various aspects of expansion such as the size, time, and technology of the newly installed dispatchable units. In TEP, the network capacity is expanded by installing new lines in order to ensure system flexibility. The location, time, and the number of the new lines are optimally determined considering the system reliability criteria [4].

The market of wind and solar PV experiences unprecedented growth in the last decade due to renewable energy polices. In the near future, some states aim to achieve a target renewables portfolio standard (RPS), where utilities have to ensure that a percentage from the electricity, they sell comes from renewable energy resources. For instant, Hawaii requires to accomplish 100% RPS by 2045 [5]. A study is presented in [6] to evaluate the integration of 50% renewables to meet the renewables portfolio standard (RPS) in California in 2030. In [7], authors study the operation and the benefits of 25% solar energy penetration in the Western Interconnection, which is a large portion of the WECC operated by a group of utilities in Arizona, Colorado, Nevada, New Mexico, and Wyoming. The paper concludes that it is operationally feasible by the Western Interconnection to adopt 25% solar energy penetration if specific operational practices and infrastructure changes are applied to the grid. A study conducted by the National Renewable Energy Laboratory (NREL), titled “the Eastern Renewable Generation

* Corresponding author.
E-mail address: msanazi@ju.edu.sa (M. Alanazi).

https://doi.org/10.1016/j.ijepes.2019.105723
Received 15 May 2019; Received in revised form 4 October 2019; Accepted 19 November 2019

Nomenclature

Indices:

t	index for year
h	index for hour
q	index for day
s	superscript for solar PV
b,m,n	index for bus
j	index for dispatchable units, and transmission lines
E	index for existing units and lines
C	index for candidate units and lines
$\sim$	index for forecasted parameters
$\hat{}$	index for known variables

Sets:

EG	set of existing dispatchable units
EL	set of existing transmission lines
CL	set of candidate transmission lines
CG	set of candidate dispatchable units
G_b	set of dispatchable units connected to bus b
L_b	set of transmission lines connected to bus b

Parameters:

B	bus-line incidence matrix
X	transmission line reactance
IC	capital cost ($)
d	discount rate
L	large positive number
D	load demand (MW)
CT	construction and commissioning time (year)
RU	dispatchable unit ramp up rate (MW/h)
RD	dispatchable unit ramp down rate (MW/h)
c	marginal generation cost ($/MWh)
α	normalized forecasted solar output
ε	small positive and predefined threshold
δ	target annual solar PV generation curtailment (MWh)

Variables:

$P^{\max}$	maximum unit generation output (MW)
Γ	operation cost ($)
P	unit generation output (MW)
P^s	solar PV capacity (MW)
PL	line flow (MW)
SL_1,SL_2	nonnegative slack variables (MW)
y	investment state (0 or 1)
θ	voltage angle
λ,π	dual variables

Integration Study (ERGIS)" investigates the impact of 30% renewable energy (solar and wind) penetration on the Eastern Interconnection (EI) [8]. The study exhibits the technical potential for EI to accommodate up to 400 GW solar and wind generation.

In the past decade, an extensive research has been conducted on how to optimally size and integrate solar PV in the distribution grid, which is referred to as hosting capacity. In [9], an optimization-based method is presented to determine the hosting capacity for distributed generation (DG) resources including solar PV, considering various performance measures. The use of active and reactive power control strategies to increase the hosting capacity through testing different solar PV inverters is demonstrated in [10]. The study in [11] presents a dynamic solar hosting capacity calculation in microgrids in case of transition from the grid-connected mode to the islanded mode. More hosting capacity studies can be found in [12–15].

The problem of generation and transmission expansion planning has been investigated in many previous studies. Authors in [16] provide a framework to analyze transmission expansion planning problem from various perspectives including mathematical models and fundamental concepts, available software tools, and educational opportunities. The study in [17] proposes two models to evaluate output power associated with large-scale wind turbines and solar PV. A probabilistic generation expansion planning model is studied in [18] while taking solar PV variability and generator outage possibility into account. This study, however, does not consider unit commitment and transmission line limits. The effect of solar PV penetration on system reliability is investigated in [19], where it concludes that strict performance requirements are needed in case of high solar PV penetration to keep the system reliable. The study in [20] analyzes the impact of large-scale wind and solar PV on net load, where it shows that negative net load

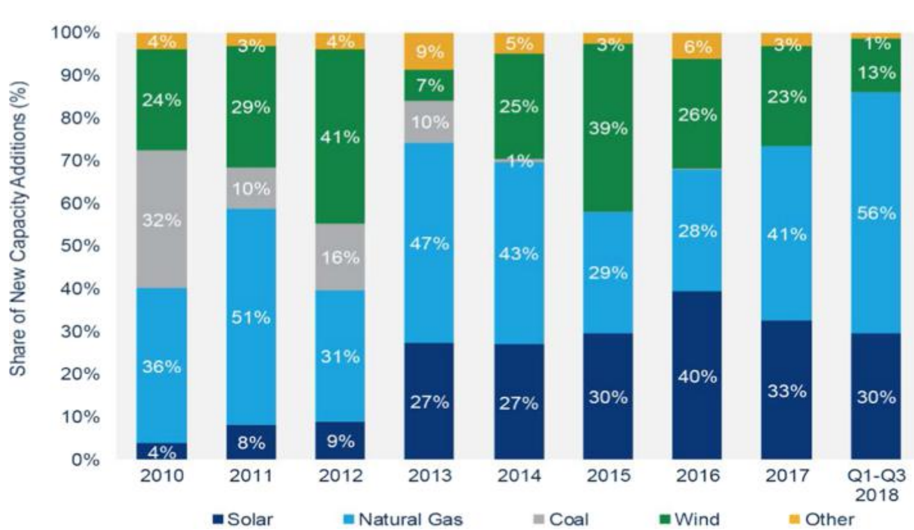

Fig. 1. Quarterly solar PV installation in the U.S. [1].

leads to renewable generation curtailment. Authors in [21] highlight the effect of DERs on design, operation, and regulation of transmission systems.

Although extensive research exists on generation and transmission expansion planning problem, only a few studies are available in the literature in which the concept of large-scale solar PV planning is discussed. The study in [22] presents an optimization-based model for large-scale solar PV planning from a private investor perspective so as to pave the way for the investor in making decisions for PV sitting, sizing, and the time of investment. Leveraging a Differential Evolution algorithm, the study in [23] proposes a least-cost generation expansion planning model with solar power plants. Ref. [24] studies large-scale solar PV in order to address economic, energy security and environmental challenges confronting power systems. A probabilistic generation portfolio modelling tool is further presented with the objective of minimizing cost and CO_2 emission.

The problem of generation and transmission expansion planning is to some extent similar to the concept of capacity expansion models. Capacity expansion models aim at simulating generation and transmission capacity investment, making assumptions about the future of electricity demand, fuel prices, technology cost and performance, as well as policy and regulation. However, the work in this paper focuses in maximizing the solar PV hosting capacity through the investment in building new dispatchable units and transmission lines considering the operational constraints. This paper proposes a co-optimization generation and transmission expansion planning model with the objective of maximizing large-scale solar PV hosting capacity. In the proposed model, dispatchable units and transmission lines are expanded in a way that the system will be able to host maximum possible solar PV. A decomposition approach is applied to coordinate planning and operation problems, and further to ensure the computational efficiency of the proposed model.

The main contribution of this paper is to provide a comparison on how generation and transmission expansion planning model optimizes solar photovoltaic generation and the associated system costs when the model is restricted to only transmission expansion and/or dispatchable generation expansion.

The rest of the paper is organized as follows. Section 2 presents the model outline for the proposed co-optimization model. The problem formulation is presented in Section 3. The effectiveness of the proposed model is investigated in Section 4 through numerical simulations on test systems, and Section 5 concludes the paper.

2. Co-optimization generation and transmission planning model outline

Fig. 2 depicts the proposed co-optimization generation and transmission planning model for maximizing large-scale solar PV capacity. The objective of this problem is to minimize the aggregated investment, for new dispatchable units and transmission lines, and system operation costs. The planning problem aims at providing new dispatchable units and transmission lines required for increasing PV hosting capacity. In other words, the system is upgraded to maximize the amount of solar PV that can be integrated to the grid. The objective is subject to prevailing operation and planning constraints associated with dispatchable units, transmission lines, and solar PV, which will be discussed in detail in the next section.

The planning problem is analyzed on an annual basis. A year is broken down into several days at which the maximum solar variability is expected to occur. The reason to select the days with maximum variability is to test the system against the worst-case scenario of generation variability as well as the ability of the system to dispatch controllable units to mitigate these variabilities. An average or a weighted profile will show much less variability so it would result in higher PV penetration results. In practice, however, if the system is designed for a weighted profile but a worse case happens, the system will not be able

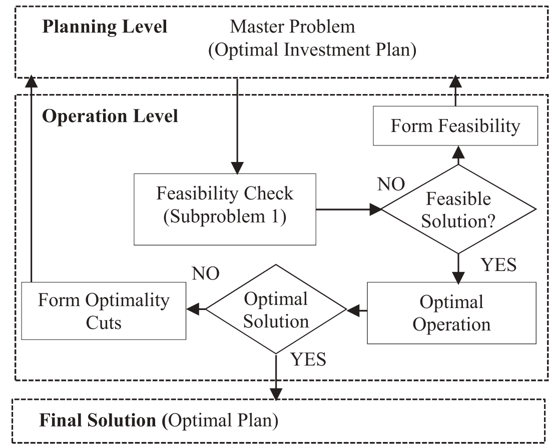

Fig. 2. The architecture of the proposed planning model.

to manage the realized PV penetration. To address this issue, a worse-case analysis, based on the maximum variability, is considered. The number of days is regarded as a tradeoff between the computational complexity and the accuracy of the proposed planning model. The Benders decomposition method is applied to mitigate with the computational complexity of the proposed problem. Benders decomposition is widely applied in long-term expansion planning problems as discussed in [25,26]. In this paper, the planning problem is decomposed into a master problem and two subproblems. The master problem determines optimal investment plan for new dispatchable units and transmission lines, and the subproblems provide feasibility check and optimal operation.

The optimal plan determined in the master problem is sent to the subproblems. The first subproblem will minimize the system network violations based on the calculated plan. If the feasibility check fails in subproblem 1, a feasibility cut is formed and sent back to the master problem to revise the solution of the next iteration of the master problem. The optimal operation is calculated in subproblem 2. In this subproblem, the operation cost is minimized considering the prevailing system operation constraints. The optimality is checked by calculating the upper bound of the original planning problem and comparing it with the lower bound which comes from the master problem. If the solution is not optimal, an optimality cut is generated and added to the master problem for the next iteration. This process will continue iteratively until a secure and optimal planning solution is achieved.

Capacity factor is one of the key factors associated with solar PV sizing. Capacity factor for solar PV is the amount of energy produced by solar PV in a year divided by the total hypothetical energy if it could produce at its nameplate capacity [27]. Due to climate conditions and zero solar irradiance at nighttime, solar PV is commonly operated at low capacity factors ranging from 10% to 25% [28]. Another decisive factor in integrating large-scale solar PV is its generation variability. Due to sudden changes in solar PV generation, the system operator may not be able to accommodate the variabilities which leads to curtailing some of the PV generation or even system performance degradation. In order to represent the capacity factor of solar PV as well as its variability in the planning model, a normalized forecast-based solar generation is used. This normalized solar generation is obtained from long-term forecasts, where to find the actual PV generation, this normalized generation is multiplied by the PV installed capacity.

3. Problem formulation

The objective of the proposed model is to minimize the planning cost of new dispatchable units and transmission lines required for increasing large-scale solar PV capacity. The planning cost of the new solar PV is ignored in this paper and only the planning cost to upgrade the system in order to accommodate more solar PVs is considered. This way it can be ensured that the problem will maximize solar PV capacity. The objective function consists of the investment cost of new dispatchable units, new transmission lines, as well as the system operation cost over the planning horizon. The ultimate solution for this problem is the installation time and size of new system upgrades as well as the maximum possible large-scale solar PV capacity. The solution steps are as follows:

3.1. Step 1 (optimal investment plan)

The first step is to calculate the optimal investment plan and projected operation cost in the master problem (MP) as shown in (1). By ignoring the investment cost of new large-scale solar PVs, the system aims at maximizing the installed solar PV. The size and the location of the expanded dispatchable units and transmission lines are optimally determined by the model in each year. $\kappa t = 1/(1 + d)^{t-1}$ is the present-worth value coefficient, introduced to evaluate the objective function in terms of a discounted cost. The projected operation cost will be achieved from the optimality cuts calculated in the optimal operation subproblem. This term will be considered zero in the first iteration.

This objective function is subject to investment constraints (2)–(4). The construction and commissioning time associated with installing new dispatchable units and transmission lines are considered in (2). To ensure there is no recurrence in calculating the capital cost, once a candidate is installed, the corresponding investment state will be fixed to 1 for the remainder of the planning horizon as in (3). The total installed solar PV capacity at each year should be greater than or equal to the installed solar PV size in the previous year as in (4).

$$\min MP$$

$$MP \geqslant \sum_t \sum_{j\in CG\,\cup\,CL} \kappa_t IC_j P_{jt}^{max,C}(y_{jt} - y_{j(t-1)}) + \sum_t \kappa_t \Gamma_t \tag{1}$$

$$y_{jt} = 0 \quad \forall\, t < \mathrm{CT_j} \ \ ,\forall\, j \in \mathrm{CG,CL} \tag{2}$$

$$y_{j(t-1)} \leqslant y_{jt} \quad \forall\, j \in \mathrm{CG,CL},\ \forall\, t \tag{3}$$

$$P^s{}_{b(t-1)} \leqslant P^s{}_{bt} \quad \forall\, b,\ \forall\, t \tag{4}$$

At high solar PV penetration, the system is expected to experience over-generation which accordingly jeopardizes the system load-supply balance. To tackle this obstacle, generation curtailment may be required in the system. Although the curtailment reduces the capacity factor and the economic viability of the renewable resource, it can alleviate the over-generation and balance the system. Curtailment can be as a result of over-generation (i.e., the renewable generation exceeds the demand), congestion in transmission lines, or voltage and interconnection issues. The Electric Reliability Council of Texas ERCOT curtailed around 17% of wind generation in 2009 [29]. In 2014, ERCOT completed a project to add new transmission lines of a capacity of 19 GW in order to accommodate the expansion in the renewable energy resources [30]. The CAISO predicts at 40% and 50% RPS, the generation curtailment is about 6.5% and 9% of renewable output, respectively [29]. The curtailment of variable energy resources can be reduced by including a battery energy storage systems (BESS). In [31], 99% reduction in wind energy curtailment is achieved by including a BESS.

3.2. Step 2 (feasibility check)

Once the optimal planning decisions for installing new dispatchable units and transmission lines are made in the master problem, the new system topology is sent to subproblem 1 to examine the feasibility of the proposed plan. This task is accomplished by minimizing the potential power mismatches via introducing two nonnegative slack variables to the load balance equation at each bus. The objective is to minimize the system violations based on the master problem solution by minimizing the sum of these slack variables as in (5).

Eq. (6) shows load balance equation at bus b, where SL1 and SL2 represent virtual generation and virtual load, respectively, where virtual load translates to generation curtailment meaning. Since there is no energy storage system incorporated in the problem, a generation curtailment from solar PV is expected especially at higher solar PV penetrations. The investment states associated with dispatchable unit and transmission line as well as the optimal size of solar PV are obtained from the optimal planning master problem. These calculated variables are substituted for local variables in order to obtain related dual variables (7) and (8). This problem is further subject to existing and candidate dispatchable unit and transmission line constraints. These constraints represent the capacity of existing and candidate dispatchable units (9) and (10), and the existing and candidate units ramp up and ramp down rate limits (11) and (12). The DC power flow calculation for the existing and candidate lines is presented in (13) and (14), respectively. The existing and candidate transmission line flows are respectively presented in (15) and (16). The phase angle of reference bus is set to zero as in (17).

$$\text{Min } r_t = \sum_q \sum_h \sum_b (SL_{bhqt,1}+SL_{bhqt,2}) \tag{5}$$

$$\sum_{j\in G_b} P_{jhqt} + \sum_{j\in L_b} PL_{jhqt} + \tilde{\alpha}_{bhqt}\hat{P}^s{}_{bt} - D_{bhqt} + SL_{bhqt,1} - SL_{bhqt,2} = 0 \quad \forall\, b,\ \forall\, h,\ \forall\, q \tag{6}$$

$$y_{jt} = \hat{y}_{jt} \leftrightarrow \lambda_{jt} \quad \forall\, j \in \mathrm{CG,CL} \tag{7}$$

$$P^s{}_{bt} = \hat{P}^s{}_{bt} \leftrightarrow \pi_{bt} \quad \forall\, b \tag{8}$$

$$0 \leqslant P_{jhqt} \leqslant P_j^{max,E} \quad \forall\, j \in \mathrm{EG},\ \forall\, h,\ \forall\, q \tag{9}$$

$$0 \leqslant P_{jhqt} \leqslant P_j^{max,C}\hat{y}_{jt} \quad \forall\, j \in \mathrm{CG},\ \forall\, h,\ \forall\, q \tag{10}$$

$$P_{jhqt} - P_{j(h-1)qt} \leqslant RU_j \quad \forall\, j \in \mathrm{EG,CG},\ \forall\, h,\ \forall\, q \tag{11}$$

$$P_{j(h-1)qt} - P_{jhqt} \leqslant RD_j \quad \forall\, j \in \mathrm{EG,CG},\ \forall\, h,\ \forall\, q \tag{12}$$

$$PL_{jhqt} = \frac{\theta_{mhqt} - \theta_{nhqt}}{X_{mn}} \quad \forall\, j \in \mathrm{EL},\ \forall\, h,\ \forall\, q \tag{13}$$

$$\left| PL_{jhqt} - \frac{\theta_{mhqt} - \theta_{nhqt}}{X_{mn}} \right| \leqslant L(1 - \hat{x}_{jt}) \ \ \forall\, j \in \mathrm{CL},\ \forall\, h,\ \forall\, q \tag{14}$$

$$|PL_{jhqt}| \leqslant PL_j^{max,E} \quad \forall\, j \in \mathrm{EL},\ \forall\, h,\ \forall\, q \tag{15}$$

$$|PL_{jhqt}| \leqslant PL_j^{max.C}\hat{y}_{jt} \quad \forall\, j \in \mathrm{CL},\ \forall\, h,\ \forall\, q \tag{16}$$

$$\theta_{bhqt} = 0 \quad b = \mathrm{ref},\ \forall\, h,\ \forall\, q \tag{17}$$

The curtailment is included in the model by introducing the target value (δt) in the Benders cut (18). If the proposed objective in (5) is less than or equal to the target value for solar PV generation curtailment, the problem will move forward to the optimal operation subproblem. Otherwise, the Benders cut (18) will be formed and added to the master problem for the next iteration. The target value for solar PV generation curtailment is expected to increase gradually as the solar PV penetration grows through the planning horizon.

Here λ and π are dual values of constraints (7) and (8), respectively. The Benders cut (18) demonstrates that the violation could be mitigated by revising the investment plan. In other words, this cut recalculates the capacity signals for the investment of new generating units, new solar PVs, and transmission lines in case the existing ones cannot satisfy the system feasibility. Nevertheless, the iterative procedure continues until a secure plan that satisfies the system feasibility is obtained.

$$r_t + \sum_j \lambda_{jt}(y_{jt} - \hat{y}_{jt}) + \sum_b \pi_{bt}(P^s{}_{bt} - \hat{P}^s{}_{bt}) \leqslant \delta_t \ \ \forall\, j \in \mathrm{CG,CL},\ \forall\, t \tag{18}$$

3.3. Step 3 (optimality check)

After the feasibility of the calculated investment plan is ensured, the optimality of the solution will be checked in the optimal operation subproblem. The objective of the optimal operation subproblem is to minimize the operating cost as shown in (19).

$$\min Q_t = \sum_q \sum_h \sum_j \kappa_t c_{jhqt} P_{jhqt} \qquad \forall j \in \text{EG,CG} \tag{19}$$

Subject to (9)–(17) and (20).

$$\sum_{j \in G_b} P_{jhqt} + \sum_{j \in L_b} PL_{jhqt} + \tilde{\alpha}_{bhqt} \hat{P}^s{}_{bt} - \hat{S}L_{bhqt,2} = D_{bhqt} \quad \forall b, \forall h, \forall q \tag{20}$$

The load balance equation is presented in (20), where the solar PV generation curtailment calculated in Subproblem 1, and then introduced in the load balance equation.

If the proposed plan is not optimal, a Benders cut will be formed and added to the master problem for the next iteration. Leveraging the proposed Benders cut (21), the lower bound of objective function in the master problem is restricted.

$$\Gamma_t \geqslant \hat{Q}_t + \sum_j \lambda_{jt}(y_{jt} - \hat{y}_{jt}) + \sum_b \pi_{bt}(P^s{}_{bt} - \hat{P}^s{}_{bt}) \quad \forall j \in \text{CG,CL}, \forall t \tag{21}$$

An optimal solution of the co-optimization generation and transmission planning problem is calculated through the iterative process amongst the master problem and subproblems. The master problem solution is regarded as the lower bound for the optimal solution. Accordingly, the upper bound for the original problem is calculated by utilizing the result from the optimal operation subproblem as in (22). This solution provides the upper bound of the objective function of the co-optimization generation and transmission planning. This upper bound is utilized to check the optimality of the solution, so that the stopping criterion is specified on the basis of this solution. The optimal solution for the proposed problem is obtained once the lower and upper bounds are converged, according to a convergence criterion as in (23)

$$Y = \sum_t \sum_j \kappa_t IC_{jt} P_{jt}^{max,C}(y_{jt} - \hat{y}_{j(t-1)}) + \sum_t \sum_b \kappa_t IC^s (P^s{}_{bt} - \hat{P}^s{}_{b(t-1)}) + \sum_t \kappa_t \Gamma_t \qquad \forall j \in \text{CG,CL} \tag{22}$$

$$\frac{Y - MP}{Y + MP} \leqslant \varepsilon \tag{23}$$

4. Numerical simulations and discussions

Four cases based on a modified six-bus test system as shown in Fig. 3 as well as the IEEE 118-bus system are analyzed to demonstrate the effectiveness and the performance of the proposed co-optimization generation and transmission planning model. The proposed model is formulated as mixed integer linear programming (MILP) and solved in a high performance computing server with Intel Xeon E7 2.3 GHz processor and 96 GB RAM using CPLEX 12.6.

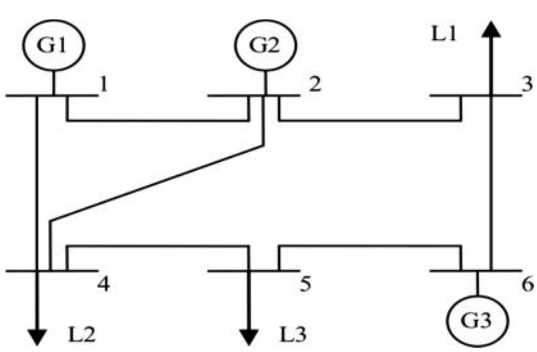

Fig. 3. IEEE Six-Bus System.

Table 1
Existing and Candidate Dispatchable unit Data of Six-bus System.

Unit No.	Bus No.	Generating Capacity (MW)	Investment Cost ($/kW)	Operation Cost ($/MWh)	Commissioning Time (Year)
1	1	100	Existing	15	–
2	2	100	Existing	18	–
3	6	50	Existing	23	–
4	1	100	200	15	3
5	2	80	270	21	2
6	2	60	250	24	2
7	3	20	250	24	1

A ten-year planning horizon is considered. The six-bus system data is available in [32]. The candidate dispatchable units and transmission lines data are provided in Tables 1, and 2, respectively, where a set of four candidate dispatchable units and four candidate transmission lines are regarded as planning options. The investment cost for solar PV is ignored to maximize its deployment. The annual load growth is considered 5% per year. The forecasted yearly peak load for the six-bus system is listed in Table 3, where the load is distributed amongst buses 3, 4, and 5 at the rate of 20%, 40%, and 40%, respectively. The data associated with the modified IEEE 118-bus system are provide in [32]. The system has 118 buses, 54 units, and 186 branches.

The solar data employed in this paper is obtained from National Renewable Energy Laboratory (NREL) for a specific location in Chicago, IL [32]. In order to reduce the computational burden, days which have worst solar PV ramping rate are considered in order to check the system ability to dispatch existing or install new dispatchable resources to mitigate these ramps.

The following cases are studied for the six-bus system:

Case 1: Solar PV integration ignoring the co-optimization generation and transmission planning.

Case 2: Solar PV integration supported by generation expansion planning.

Case 3: Solar PV integration supported by transmission expansion planning.

Case 4: Co-optimization generation and transmission planning.

An additional case is considered to study a relatively bigger test system:

Case 5: Co-optimization generation and transmission planning to support solar PV integration for the IEEE 118-bus system.

Case 1:

This case is considered as a base case for large-scale PV hosting capacity and cases 2–4 are compared to this case. The large-scale PV hosting capacity is calculated without considering any system upgrade. A total solar capacity of 123.95 MW is installed at bus 5 in year 1. Load is mainly supplied by unit 1 as the least expensive unit. Unit 2 is the next economic unit after unit 1, however it is partially dispatched due to congestion in line 2–3. As depicted in Fig. 4, the system accommodates a considerable amount of solar PV in the first six year to reach a total capacity of 162.55 MW (with a breakdown of 141.78 MW and 20.77 MW at buses 5 and 4, respectively). In year 7, however, the system has neither adequate generation to supply the load nor adequate network capacity to accommodate additional solar PV, therefore it experiences a load curtailment of 12.65 MWh as shown in Fig. 5. In the first seven years, the system experiences solar PV generation curtailment mainly due to overgeneration. However, once there is no further installation of solar PV and considering the load growth, the curtailment is reduced to zero. By the end of the planning horizon the total installed solar PV capacity reaches 163 MW which supplies 21% of the

Table 2
Existing and Candidate Transmission Line Data of Six-bus System.

Line No.	From Bus	To Bus	X (p.u)	Capacity (MW)	Investment Cost ($/kW)	Commissioning Time (Year)
1	1	2	0.17	70	Existing	–
2	2	3	0.037	70	Existing	–
3	1	4	0.258	80	Existing	–
4	2	4	0.197	80	Existing	–
5	4	5	0.037	50	Existing	–
6	5	6	0.14	80	Existing	–
7	3	6	0.018	80	Existing	–
8	1	2	0.17	70	23	2
9	2	3	0.258	70	23	2
10	2	4	0.258	80	24	2
11	3	6	0.018	70	24	2

Table 3
Forecasted Yearly Peak Load of Six-bus System.

Year	1	2	3	4	5
Peak (MW)	209	219	230	241	254
Year	6	7	8	9	10
Peak (MW)	266	280	294	308	324

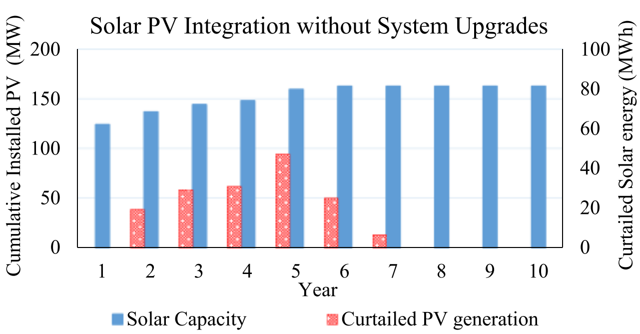

Fig. 4. Installed solar capacity and curtailed solar energy without system upgrade.

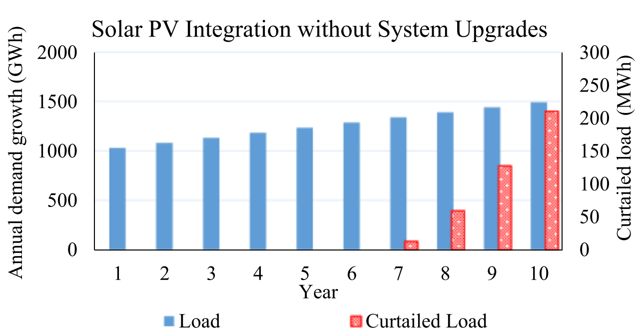

Fig. 5. Annual demand and curtailed load without system upgrade.

total annual load. Case 1 is considered as a base case for large-scale PV hosting capacity and cases 2–4 are compared to this case.

Case 2: Solar PV integration is supported by generation expansion planning in this case, i.e., the proposed planning model is used while ignoring transmission line installation. Solar PV is installed at buses 3 and 5. The load is mainly supplied by unit 1 and when solar PV generation is available, generation from both units 2 and 3 goes to zero in most times. As presrnted in Fig. 6, the system keeps accommodating more solar PV while maintaining the feasibility of transmission flows to reach a total of 157.53 MW at bus 3 in year 5. About 25% of the load supply in year 5 comes from solar PV, where the system curtails a total of 150 MWh of solar PV energy due to excess generation. In year 6, a total of 4.92 MW and 12.80 MW is installed at buses 3 and 5, respectively. In year 7, a new generation capacity needs to be installed to

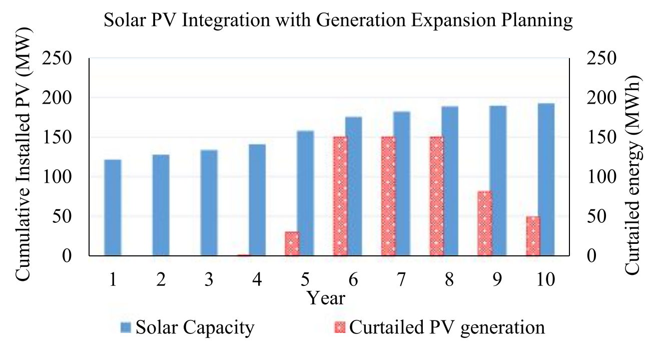

Fig. 6. Installed solar capacity and curtailed solar energy considering generation expansion planning.

satisfy the load growth especially at hours where solar PV generation is not available. In year 8, line 5–6 is congested which causes unit 2 to dispatch at its maximum capacity in order to supply the load at bus 4. Due to repeated congestion at both lines 2–3 and 5–6, the system has to curtail a total of 150 MWh of solar PV energy in year 8. In year 9, when solar PV generation is not available or low, units 1 and 2 are dispatched at their maximum capacity. Moreover, since lines 1–2, 2–3 and 5–6 are congested, a new generation needs to be installed to supply the load at bus 4. The available options are to install at bus 1 or 2. The installation of a new unit at bus 2 would cause more congestion between buses 2 and 3. As a result, the model selects unit 4 to be installed. Once candidate unit 4 is installed, unit 2 reduces its generation as it is cheaper to supply the load from the new installed unit. By the end of the planning horizon, the total installed solar PV capacity reaches 192 MW which supplies 26% of the annual load, i.e., a 5% increase compared to Case 1 at the expense of high investment cost of $ 17.3 M.

Case 3: Solar PV integration is supported by transmission expansion planning in this case, i.e., the proposed planning model is used while ignoring dispatchable unit installation. Similar to previous cases, line 2–3 often experiences a congestion, causing a reduction in generation of unit 2. In year 1, the total installed PV capacity is 122.36 MW. As presented in Table 4, candidate lines 2–3 and 1–4 are installed in the second year to increase the network capacity and hence allow more large-scale solar PV installations. In year 4, a total of 86.16 MW solar PV capacity is installed at bus 5. Also, candidate line 1–2 is installed in

Table 4
Candidate unit and line installation year for six bus-system.

	Candidate Unit				Candidate Line			
	4	5	6	7	1–2	2–3	2–4	3–6
Case 2	9	–	–	7	–	–	–	–
Case 3	–	–	–	–	4	2	2	–
Case 4	–	–	7	–	–	2	–	5

year 4 to increase the network capacity. In year 7, the system needs to install new dispatchable units to meet the demand growth; however, since no generation expansion is considered in this case, the system curtails 7.45 MWh of the load. Compared to Case 1, the load curtailment is reduced due to the increase in solar PV hosting capacity driven by the increase in the network capacity. By the end of the planning horizon, the total installed solar PV capacity is 266 MW, which supplies 34%, a much higher percentage than in previous cases. The planning cost for adding the new lines is $ 4.58 M.

Case 4: In this case, the proposed co-optimization generation and transmission planning model is employed to maximize solar PV capacity. Fig. 9 shows the annual installed solar PV over the planning horizon.

In the first year, the total installed solar PV capacity is 122.55 MW where 120.09 MW and 2.46 MW are installed at buses 5 and 6, respectively. To remove congestion in line 2–3, candidate line 2–3 is installed in year 2. Line 4–5 is congested at the first year caused by the installation of solar PV at bus 5. During nighttime hours or the unavailability of solar generation due to weather conditions, unit 1 is dispatched at its maximum capacity and the remaining is supplied by units 2 and 3. However, during the afternoon periods where solar PV generation is at its maximum, the load is supplied by solar PV as it has no operation cost. Accordingly, generation from units 1 and 2 is reduced and the generation from units 3 is dropped to zero. In year 1, 23% of the annual demand is supplied by solar PV. The total solar energy curtailed in year 1 is 30.42 MWh, which is mainly due to solar PV over-generation. In year 2, the total solar PV capacity is increased to 150.15 MW where 8.19 MW and 19.41 MW are installed at buses 5 and 6, respectively. In year 2, 27% of the annual demand is supplied by solar PV. A total of 5.3 GWh solar PV energy is curtailed in year 2 due to excess solar PV generation, representing 1.78% of its total annual energy generation.

A total of 15.04 MW of solar PV capacity is added in year 3. In year 4, an additional of 144.89 MW is installed at bus 3, supplying 39% of the annual demand. In year 5, a total of 100.69 MW solar PV is installed at bus 5 which increases the annual demand supplied by solar PV to 40%. The installed capacity of the solar PV meets the load growth which delayed any additional unit to be installed to meet the load growth. In year 5, line 3–6 experiences congestion which results in additional curtailment of solar PV generation. As a result, the candidate line 4 is installed. As the hosting capacity of the solar PV increases, the system experiences more solar PV energy curtailment due to excess generation. In year 5, the total solar PV energy curtailed over the year is 10.78 GWh. In year 6, the system accommodates more solar PV where an additional 14.86 MW is installed at bus 3. In year 7, the system needs to install new generation capacity in order to meet the load growth especially at nighttime hours when solar irradiance is not available. Considering the remaining years in the planning horizon, candidate units 6 and 7 are the available options. Unit 6 is installed as it has higher ramp up/down limits, which can manage any substantial ramps in the net load caused by the solar PV variability. At the end of the planning horizon, the solar PV reaches a total capacity of 451 MW and supplies 40% of the annual demand. The total planning cost for reinforcing the system with new lines and units is $ 14.3 M. In year 10, the total curtailed solar PV energy is 10.14 GWh, which represents 34% of the total solar PV generation.

Case 5: To demonstrate the effectiveness of the proposed model on a relatively larger system, the proposed co-optimization generation and transmission planning problem is solved for the IEEE 118-bus system. The list of existing and candidate generating units and transmission lines for the IEEE 118-bus system is available in [32]. The existing generation capacity is 7,500 MW. The peak load is 4090 MW and the load growth is considered to be 5%.

In the first year, a total of 1.35 GW of solar PV is installed. Candidate lines 80–99 and 94–100 are installed in year 1 in order to accommodate the anticipated increase in solar PV penetration. At the second year, a total of 0.8 GW is added to the system at buses 37, 56, 100 and 113 and candidate lines 8–30 and 17–113 are further installed. Candidate units 2, 3 and 11 are installed in year 2 at the buses 10, 12, and 113 in order to mitigate any ramps caused by solar PV variability. Unit 9 is installed in year 5 in order to transfer power to the loads due to congestion in line 8–5. A 2.5 GW of solar PV is added in year 6. To elevate this congestion and provide solar PV generation with sufficient access to transmission lines capacity, candidate lines 77–82 and 82–83 are installed in year 6. Also, the total curtailed solar PV energy is 2,835 GWh, which represents 23% of the generated solar PV.

The total cumulative solar PV installed by the end of the planning horizon is 7.9 GW which supplies 38% of the annual load. The total planning cost in order to maximize the solar PV hosting capacity and accommodate such large-scale of solar PV is $100 M.

5. Discussions

Table 5 summarizes the results for cases 1–4. In case 1 which is considered as the base case, neither the generation nor the transmission expansion planning are considered in the problem. The system accommodates more solar PV in the first six years to reach to total installed capacity of 163 MW by the end of year six. Due to inadequacy in the network capacity, no more solar PV is installed. Moreover, part of the load is curtailed as the load is more than the generation. In case 2, only generation explanation is considered in the problem. Reinforcing the system with only generation expansion at a cost of $17.3 M increases solar PV penetration by 5%. As the objective of the expansion problem is to minimize the planning cost, unit 4 is installed in year 7 to satisfy the load growth. In year 9, due to congestion in the lines and to supply the load at bus 4, unit 4 is installed to satisfy the load balance equation. In case 3, only the transmission expansion planning is considered. The solar PV penetration is increased by 13% and 8% compared to cases 1 and 2, respectively. As shown in Fig. 7, the total installed solar PV capacity is 266 MW by the end of the planning horizon. This increase shows that ensuring the flexibility of the grid would allow the grid to sustain more solar PV installations. By reinforcing the system with both generation and transmission expansion planning as in case 4, the model maximizes the penetration of solar PV to reach to 40% at a cost of $14.3 M. By applying the co-optimization planning model, the solar PV penetration is increased by 19%, 14%, and 6% compared to cases 1, 2, and 3, respectively.(see Fig. 8).

Table 5
Summary for Six-Bus system Cases.

	Case 1	Case 2	Case 3	Case 4
Solar PV penetration	21%	26%	34%	40%
Total Planning Cost ($ M)	0	17.3	4.58	14.3
Installed PV (MW)	163	192	266	451

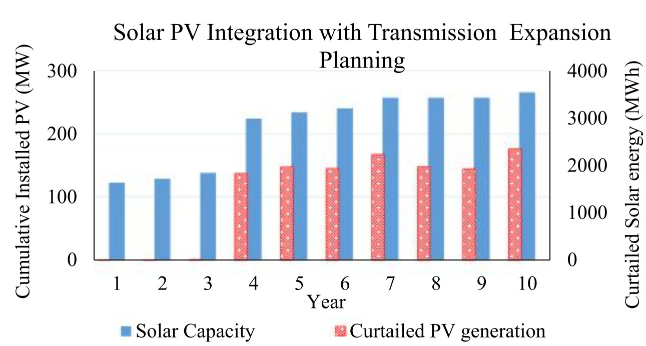

Fig. 7. Installed solar capacity and curtailed solar energy considering transmission expansion planning.

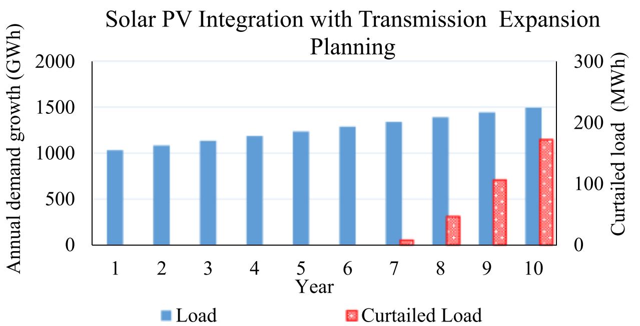

Fig. 8. Annual demand and curtailed load considering transmission expansion planning.

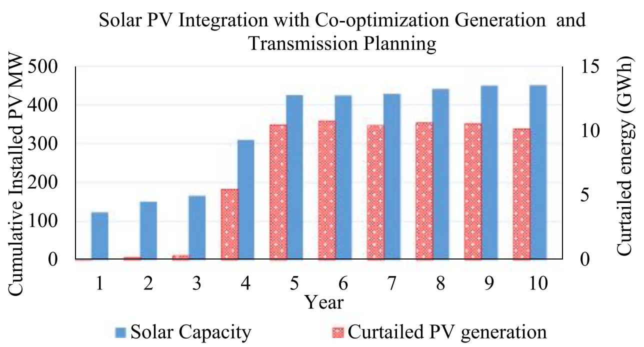

Fig. 9. Installed solar capacity and curtailed solar energy considering generation and transmission expansion planning.

6. Conclusion

In this paper, a co-optimization generation and transmission planning model was proposed to maximize large-scale solar PV integration. The Benders decomposition method was used to tackle the computational complexity of the model. The proposed model was analyzed through numerical simulations on a small-scale six-bus system as well as relatively large 118-bus test system. The obtained results exhibited that maximizing the large-scale solar PV hosting capacity necessitates a system upgrade. New transmission lines and dispatchable units were to be installed to ensure system flexibility. With proper investments in system upgrade, the studied test system could accommodate up to 40% solar PV by the end of the planning horizon. It was further concluded that reinforcing the system with only transmission lines upgrade would decrease the solar PV penetration to 34%. Moreover, the solar PV penetration would decrease by 14% when the system is only reinforced with dispatchable units upgrade, advocating that a co-optimization planning is much more effective than individual upgrades of generation and transmission. The results further advocated that solar PV energy curtailment is an inherent part of the large-scale solar PV proliferation. This energy curtailment is mainly caused by the lack of adequate system capacity, either in generation or transmission, to fully support solar PV generation, as well as potential overgeneration at times of low load.

Declaration of Competing Interest

We declare that we have no conflict of interest.

References

[1] Perea A, Honeyman C, Smith C, Rumery S, Holm A. U.S. solar market inisight executive summary Q2 2018," GTM Research and the Solar Energy Industries Associationl Jun. 2018.
[2] Alanazi M, Mahoor M, Khodaei A. Two-stage hybrid day-ahead solar forecasting. ArXiv Prepr. ArXiv170608699 2017.
[3] Alanazi M, Mahoor M, Khodaei A. Day-ahead solar forecasting based on multi-level solar measurements. In: 2018 IEEE/PES transmission and distribution conference and exposition (T&D), Denver, CO, USA, 2018, pp. 1–9.
[4] Hemmati R, Hooshmand R-A, Khodabakhshian A. Comprehensive review of generation and transmission expansion planning. IET Gener Transm Distrib Sep. 2013;7(9):955–64.
[5] Barbose G. U.S. Renewable Portfolio Standards '2018 Annual Status Report, Lawrence Berkeley National Laboratory; Nov. 2018.
[6] "Investigating a Higher Renewables Portfolio Standard in California," Energy and Environmental Economics, Inc, Executive Summary; Jan. 2014.
[7] Lew D, Miller N, Clark K, Jordan G, Gao Z. Impact of high solar penetration in the western interconnection. Contract 2010;303:275–3000.
[8] Bloom A et al. Eastern renewable generation integration study, Natl. Renew. Energy Lab. Gold. CO Tech Rep NRELTP-6A20-64472; 2016.
[9] Alturki M, Khodaei A, Paaso A, Bahramirad S. Optimization-based distribution grid hosting capacity calculations. Appl Energy 2018;219:350–60.
[10] Esmaili M, Firozjaee EC, Shayanfar HA. Optimal placement of distributed generations considering voltage stability and power losses with observing voltage-related constraints. Appl Energy 2014;113:1252–60.
[11] Hosseini ZS, Khodaei A, Paaso EA, Hossan MS, Lelic D. Dynamic solar hosting capacity calculations in microgrids. In: Presented at the CIGRE US National Committee 2018 Grid of the Futur, p. 12.
[12] Hung DQ, Mithulananthan N, Bansal RC. Analytical strategies for renewable distributed generation integration considering energy loss minimization. Appl Energy 2013;105:75–85.
[13] Georgilakis PS, Hatziargyriou ND. Optimal distributed generation placement in power distribution networks: models, methods, and future research. IEEE Trans Power Syst 2013;28(3):3420–8.
[14] Mokgonyana L, Zhang J, Li H, Hu Y. Optimal location and capacity planning for distributed generation with independent power production and self-generation. Appl. Energy 2017;188:140–50.
[15] Capitanescu F, Ochoa LF, Margossian H, Hatziargyriou ND. Assessing the potential of network reconfiguration to improve distributed generation hosting capacity in active distribution systems. IEEE Trans Power Syst 2015;30(1):346–56.
[16] Quintero J, Zhang H, Chakhchoukh Y, Vittal V, Heydt GT. Next generation transmission expansion planning framework: models, tools, and educational opportunities. IEEE Trans Power Syst 2014;29(4):1911–8.
[17] Marinelli M, Maule P, Hahmann AN, Gehrke O, Norgard PB, Cutululis NA. Wind and photovoltaic large-scale regional models for hourly production evaluation. IEEE Trans Sustain Energy 2015;6(3):916–23.
[18] Munoz FD, Mills AD. Endogenous assessment of the capacity value of solar PV in generation investment planning studies. IEEE Trans Sustain Energy 2015;6(4):1574–85.
[19] Achilles S, Schramm S, Bebic J. Transmission system performance analysis for high-penetration photovoltaics," NREL/SR-581-42300, 924641; Feb. 2008.
[20] Shaker H, Zareipour H, Wood D. Impacts of large-scale wind and solar power integration on California's net electrical load. Renew Sustain Energy Rev 2016;58:761–74.
[21] Perez-Arriaga IJ. The transmission of the future: the impact of distributed energy resources on the network. IEEE Power Energy Mag 2016;14(4):41–53.
[22] Muneer W, Bhattacharya K, Canizares CA. Large-scale solar PV investment models, tools, and analysis: The Ontario Case. IEEE Trans Power Syst 2011;26(4):2547–55.
[23] Rajesh K, Bhuvanesh A, Kannan S, Thangaraj C. Least cost generation expansion planning with solar power plant using Differential Evolution algorithm. Renew Energy 2016;85:677–86.
[24] Vithayasrichareon P, MacGill IF. Valuing large-scale solar photovoltaics in future electricity generation portfolios and its implications for energy and climate policies. IET Renew Power Gener 2016;10(1):79–87.
[25] Shahidehpour M, Fu Y. Benders decomposition in restructured power systems. IEEE Power Energy Mag. 2005;3(2):20–1.
[26] G. A.M. Generalized benders decomposition 1972;10 (4): p. 237–60.
[27] Madaeni SH, Sioshansi R, Denholm P. Comparison of capacity value methods for photovoltaics in the Western United States," NREL/TP-6A20-54704, 1046871; Jul. 2012.
[28] "EIA" U.S. Energy Information Administration, "Electric Power Monthly with data for November 2018,"; 2019. p. 274.
[29] Bird L, Cochran J, Wang X. Wind and solar energy curtailment: experience and practices in the United States," NREL/TP–6A20-60983, 1126842; Mar. 2014.
[30] Lasher W. The competitive renewable energy zones process; 2014. p. 12.
[31] Alanazi A, Khodaei A. Optimal battery energy storage sizing for reducing wind generation curtailment. In: Presented at the Power & Energy Society General Meeting 2017 IEE; 2017. p. 1–5.
[32] "National Solar Radiation Data Base". https://rredc.nrel.gov/solar/old_data/nsrdb/ [Online].